

Active Vibration Control Analysis of Cantilever Pipe Conveying Fluid Using Smart Material

Prof.Dr. Muhsin J.Jweeg¹, *Thaier J.Ntayeesh²

1. Mechanical Engineering Department, AL_Nahrain University, Baghdad, Iraq

2. Mechanical Engineering Department, University of Baghdad, Baghdad, Iraq

Abstract

In this paper, experimental and simulation studies in active vibration of smart cantilever pipe conveying fluid have been presented to investigate the open and closed loop time responses.

A program to simulate the active vibration reduction of stiffened pipe with piezoelectric sensors and actuators was written in the ANSYS workbench and Parametric Design Language (APDL). This makes use of the finite element capability of ANSYS and incorporates an estimator based on optimal linear quadratic control (LQR) schemes to investigate the open and closed loop time responses. The procedures are tested by active control for free and forced vibrations of piezoelectric smart cantilever pipe conveying fluid. Harmonic excitation is considered in the forced vibration.

Experiments have been done to verify with simulations. Smart pipe consists of aluminum pipe surface glued piezoelectric patches of MIDÉ QuickPack QP20W transducers. An experimental result is acquired by LabVIEW programs.

It is found the location of the piezoelectric actuator has influence on the response of the cantilever pipe. The displacement increases when the actuators are moved closer to the clamped. This is due to the higher strain developed near the clamped.

The control performance decrease with increasing the flow velocity due to increased coriolis force. The better performance of control occur at minimum velocity ($Q=10L/min$) and location of actuator, the maximum reduced the displacement response from +8mm to 1mm.

Keywords: Active vibration control, LQR, cantilever pipe, smart structure, Smart material, piezoelectric.

1. Introduction

Pipes conveying fluid are of considerable interest in many engineering fields. They are widely used in various industrial branches. Sometimes, their role is simply to transport fluids, as in oil pipelines, pump discharge lines, propellant lines and municipal water supply. In other cases, they provide basic structural components as in power plants, chemical plants, hydraulic systems, chemical plants, liquid-fuel rocket piping components, refrigerators, air-conditioners, heat exchangers, and so on.

In general, the dynamical behavior of pipes conveying fluid are more complicated than the corresponding structure without fluid. In the latter case, free vibrations for a specified structure (degree of freedom and boundary conditions) depend only on its mass and stiffness. In such structures the Eigen values are related to structure parameters, hence the natural frequency is unique. In this case the vibrations are of uncontrolled type. If however, such structures are subjected to an axial force, it is seen that the Eigen values are affected by the amount and direction of this force. In other words if this force is compressive the natural frequencies decrease with the increasing of this force. In this case vibration is controlled by this force and there is a critical value of this force at which the fundamental frequency drops to zero leading to buckling state.

A large number of articles at home and abroad focus on pipes conveying fluid and flexible beam structure vibration control field. For example, [1] and [2] introduced independent mode space concept in optimal control and model reference self-adaptation control, and adopt ceramic piezoelectric sheets as simulator to control cantilever pipes conveying fluid vibration under steady flow. [3] Conducted active control on nonlinear restrains cantilever pipes conveying fluid vibration under steady flow with ceramic piezoelectric sheets as simulator. [4] Conducted active control on fixed at both ends of pipes vibration under over critical velocity steady flow based on optimal independent mode space control method with ceramic piezoelectric sheets as simulator. [5] studied cantilever pipes conveying fluid vibration control under steady flow, and flexible cantilever beam vibration control.

All of above articles used ceramic piezoelectric sheets as simulator. These articles showed ceramic piezoelectric sheets have been widely applied for control simulator and mode sensor design. Using ceramic piezoelectric sheets as mode sensor takes the advantage of direct piezoelectric effects of piezoelectric ceramic. Direct piezoelectric effects refer to some mediums deformations under force due to lack of symmetric centre, and caused surface electrification. On the contrary, adding exciting electric field will cause mechanical deformations, which calls inverse piezoelectric effects. Based on this feature, ceramic piezoelectric sheets are designed as simulator.

2. Methods of Vibration Reduction

Mechanical vibration can be reduced using passive, semi-active and active vibration reduction methods based on the type of problem involved. Stiffening, damping and isolation are considered as the main methods used to suppress vibration passively. The mechanical structure can be stiffened and changed inherently by adding beam stiffeners or increasing layers in the structure of the same material or a different material as in composites. This stiffening shifts the structural resonance frequency beyond the band of excitation frequency in order to reduce the effects of resonance. This method works effectively if the band of external excitation frequency is known.

A damper can be added to a structure in order to reduce structural resonance peaks by dissipating the vibration energy through the damper. Damping can be achieved passively with fluid dampers, eddy currents, elastomer elements or by diverting dynamic energy from the main structure to the dynamic vibration absorber. Vibration.

energy can also be converted to electrical energy using transducer and dissipated into electrical network or stored as harvested energy [6].

A number of studies presented by Manjunatah et al showed that smart materials, such as piezoelectric, magneto-rheological fluids and shape memory alloys, mounted with a mechanical structure can produce a second response which interacts with the first mechanical structure's response in order to improve the overall response [7].

The literature identifies three important points about active vibration control of flexible structures: firstly, the importance of using discrete rather than distributed sensor/actuator; then the need to find optimal locations for the sensor/actuators on a structure rather than locating them randomly; and finally the type of control scheme has a significant effect on the effectiveness of the sensor/actuators for vibration suppression.

3. Control Scheme

Classical direct proportional feedback, negative-gain velocity feedback and optimal linear quadratic control schemes have been implemented in several studies [8, 9, 10,11] to attenuate vibration in flexible structures and it has been reported that optimal linear quadratic control gives higher effective and lower actuator peak voltage than the classical approach. Active vibration control was investigated by Kapuria and Yasin for a cantilever fibre reinforced plate fully covered with multi-segment piezoelectric sensors/actuator pairs. It was found that this multiple piezoelectric segmentation gives faster vibration suppression for the same gain in classical direct feedback control and for the same output weighted parameters of the optimal linear quadratic control [12].

Vibration suppression of a composite cantilever beam with a single sensor/actuator pair bonded near the beam root was investigated theoretically and experimentally by Zabihollah et al using an optimal linear quadratic control scheme. They said that this is most efficient control scheme to find the optimal feedback control gain matrix [13].

Active vibration suppression in a fully clamped composite plate with five randomly located piezoelectric pairs using an optimal linear quadratic control scheme was investigated by Uyanik. He reported that the active damping may become unstable as a result of large values in the control gain matrix and that it is necessary to explore the optimum feedback gain matrix in order to suppress vibration effectively with stable active damping [14]. In an optimal linear quadratic control scheme, the optimum feedback control matrix is related to the optimal location of actuators.

Han and Lee experimentally investigated active vibration control of a cantilever plate by optimally placed sensors and actuators using classical proportional feedback control and this significantly suppressed vibration at the first five modes [15].

The literature identifies three important points about active vibration control of flexible structures: firstly, the importance of using discrete rather than distributed sensor/actuator; then the need to find optimal locations for the sensor/actuators on a structure rather than locating them randomly; and finally the type of

control scheme has a significant effect on the effectiveness of the sensor/actuators for vibration suppression.

In this study, an optimal linear quadratic control scheme was implemented to optimize the discrete piezoelectric actuators and controller feedback gain matrix in order to suppress vibration effectively.

The modeling of a smart cantilever pipe conveying fluid using the finite element method produces many hundreds or thousands of coupled equations and requires a large computational effort to study the response of the first modes.

4. Modal Structure

The active control of a smart cantilever pipe under free and forced vibration is analyzed at different actuators locations using LQR method of control. The aluminum smart pipe is composed of Five piezoelectric (Lead-Zirconate-Titanate) patches. Three of the piezoelectric patches is used as controlling actuator in different position and the other two piezoelectric patch are used as vibration generating shaker for forced vibration and sensor. The three PZT actuators (1,2,3) are placed 0.5, 21.7, 45.7cm away from the root respectively. The PZT shaker and sensor are placed 11.4,33.7cm away from the root respectively at the opposite side of the pipe as shown in Fig.(1). The dimensions and material properties of the smart pipe and piezoelectric are shown in Table(1).

4. Finite Element Method

It is possible to model smart structures with piezoelectric materials by ANSYS/ Multi physics product. In this chapter, the integration of control actions to the ANSYS solution is realized. The smart structures are studied by ANSYS version 15. In order to improve the demonstration hardware, this work required to investigate the behavior of the AVC laboratory structure in different design versions. The material and dimensions of the pipe and more importantly the placement and configuration of the sensors was also explored by means of FE simulations. Each of these design iterations required to take the modal, transient and frequency response of the system into account. The choice FE software to carry out simulations was ANSYS. This software provides readily available elements for multidisciplinary simulations. Amongst others, there are elements with piezoelectric properties suitable to prepare models of active structures.

The simulation divided to two steps, the first step was the use of FSI. The fluid pressure results from ANSYS FSI can be easily transferred into second step (APDL) analysis as shown in the following stage.

5.1 ANSYS Workbench Solvers for the FSI

In this section a numerical analysis was adopted by using finite element approach (FEA) to calculate vibration characteristics of pipe conveying fluid using a general purpose package ANSYS V15.0. Workbench comes into its own when it comes to build multi-stage workflows, where separate analysis systems work together as shown in Fig. (2). It can start with a fluid flow simulation to find the pressure fluctuation in inner surface of pipe. These pressures can then be automatically applied to a structural analysis simulation to find the performance of the parts in question.

In simulation terms this type of analysis is extremely complex. Most fluid flow simulation technology uses completely different meshing, loading and solving methods compared to structural simulation. The software has the ability to transform meshes between the two disciplines and to ensure that parameters and variables remain consistent where needed. Modal analysis also used in workbench to determine the vibration characteristics (natural frequencies and mode shapes) of a structure. The approach is divided into four parts: computational fluid dynamics (CFD), structure analysis, coupled field fluid-structure analysis and modal analysis.

The fluid pressure results from ANSYS FSI can be transferred into second step (APDL) analysis.

In an unstressed one-dimensional dielectric medium, the electric displacement D (charge per unit area, expressed in C/m^2) is related to the electric field E (V/m) by

$$D = \epsilon E \quad (1)$$

where ϵ is the dielectric constant of the material. Similarly in a one dimensional elastic body placed in a zero electric field, the strain S and the stress T (N/m²) are related by

$$S = sT \quad (2)$$

where s is the compliance of the material (inverse of the Young modulus). For a piezoelectric material, the electrical and mechanical constitutive equations are coupled.

$$S = d^T T + \epsilon^T E \quad (3)$$

$$D = \epsilon^T T + \epsilon^S E \quad (4)$$

In Equation (3), the piezoelectric constant d relates the strain to the electric field E in the absence of mechanical stress and ϵ^T refers to the compliance when the electric field is constant. In Equation (4), d relates the electric displacement to the stress under a zero electric field (short circuit electrodes); d is expressed in (m/V or Coulomb/Newton). ϵ^T is the dielectric constant under constant stress. The above equations can be arranged into [16].

$$T = \frac{1}{s^E} S - \frac{d}{s^E} E$$

$$D = \frac{d}{s^E} S + \left(1 - \frac{d^2}{s^E \epsilon^T}\right) E$$

which are usually rewritten as

$$T = c^E S - e^T E$$

$$D = e^S S + \epsilon^T (1 - k^2) E$$

where $c^E = 1/s^E$ is the Young's modulus under constant electric field (in N/m^2); $e^T = d/s^E$ is the constant relating the electric displacement to the strain, for short circuited electrodes (in Coulomb/ m^2).

$k^2 = d^2/(s^E \epsilon^T)$ is called the coupling coefficient of the piezoelectric material. This name comes from the fact that, at frequencies far below the mechanical resonance frequency of the piezoelectric, is expressed as [16].

$$k^2 = \left(\frac{\text{stored energy converted}}{\text{stored input energy}} \right)$$

A high value of k is desirable for efficient transduction. From Equation (8), the dielectric constant under constant strain is related to that under constant stress by . Equation (8) is the starting point for the formulation of the equation of a laminar piezoelectric actuator, while Equation (7) is that for a laminar sensor. Fig. (3) shows the laminar design of the piezoelectric actuator [16].

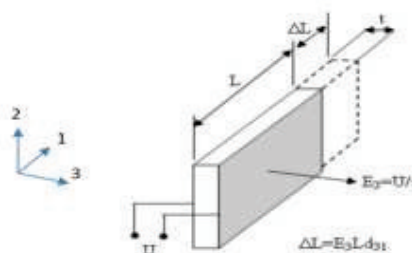


Fig.(3): laminar designs (d31)

If the direction of the polarization coincides with direction 3, the constitutive equations for the actuation and sensing mechanisms can be rewritten in matrix form: [16]

$$\begin{Bmatrix} S_{11} \\ S_{22} \\ S_{33} \\ 2S_{23} \\ 2S_{13} \\ 2S_{12} \end{Bmatrix} = \underbrace{\begin{bmatrix} s_{11} & s_{12} & s_{13} & 0 & 0 & 0 \\ s_{12} & s_{22} & s_{23} & 0 & 0 & 0 \\ s_{13} & s_{23} & s_{33} & 0 & 0 & 0 \\ 0 & 0 & 0 & s_{44} & 0 & 0 \\ 0 & 0 & 0 & 0 & s_{55} & 0 \\ 0 & 0 & 0 & 0 & 0 & s_{66} \end{bmatrix}}_{\text{compliance}} \begin{Bmatrix} T_{11} \\ T_{22} \\ T_{33} \\ T_{23} \\ T_{13} \\ T_{12} \end{Bmatrix} + \underbrace{\begin{bmatrix} 0 & 0 & d_{31} \\ 0 & 0 & d_{32} \\ 0 & 0 & d_{33} \\ 0 & d_{24} & 0 \\ d_{13} & 0 & 0 \\ 0 & 0 & 0 \end{bmatrix}}_{\text{coupling}} \begin{Bmatrix} E_1 \\ E_2 \\ E_3 \end{Bmatrix}$$

Sensing:

$$\begin{Bmatrix} D_1 \\ D_2 \\ D_3 \end{Bmatrix} = \underbrace{\begin{bmatrix} 0 & 0 & 0 & 0 & d_{15} & 0 \\ 0 & 0 & 0 & d_{24} & 0 & 0 \\ d_{31} & d_{32} & d_{33} & 0 & 0 & 0 \end{bmatrix}}_{\text{coupling}} \begin{Bmatrix} T_{11} \\ T_{22} \\ T_{33} \\ T_{23} \\ T_{13} \\ T_{12} \end{Bmatrix} + \underbrace{\begin{bmatrix} \epsilon_{11} & 0 & 0 \\ 0 & \epsilon_{22} & 0 \\ 0 & 0 & \epsilon_{33} \end{bmatrix}}_{\text{permittivity}} \begin{Bmatrix} E_1 \\ E_2 \\ E_3 \end{Bmatrix}$$

Examining the actuator equation (4.9), when an electric field is applied parallel to the direction of polarization, an extension is observed along same direction; its amplitude is governed by the piezoelectric coefficient d_{33} . Shrinkage is observed along the direction 1 and 2 perpendicular to the electric field, the amplitude of which is controlled by d_{31} and d_{32} respectively. Piezoceramics have an isotropic behavior in the plane $d_{31} = -d_{32}$. Equation (4.9) also indicates a shear deformation s_{13} controlled by the piezoelectric constant d_{15} (the same occurs if a field E_1 is applied) [16].

5.2 Element Type:

I. Pipe Element

The models pipe which are used should be discretized to small elements for finite element analysis the element type that is used in this discretizing is SOLID45, it is used for the 3-D modeling of solid structures. The element is defined by eight nodes having three degrees of freedom at each node: translations in the nodal x, y, and z directions. The element has plasticity, creep, stress stiffening large deflection, and large strain capabilities [17].

II. Piezoelectric Element

ANSYS FE-program offers two and three dimensional piezoelectric coupled-field elements for modeling structures with piezoelectric actuators/sensors. Static, modal, full harmonic and transient analysis can be performed with this commercial software. Plane and solid piezoelectric elements are available in ANSYS. They have the capability of modeling piezoelectric response.

For a piezoelectric element there are four DOF at each node; u_x , u_y , u_z and volt. In this case, it is necessary to use 'coupled-field analysis' to couple the interaction between applied stress and electric field. The choice between these five coupled field elements is dependent on the sample geometric model. In this thesis, the brick-shaped element SOLID5 is chosen due to the fact that the geometrical shape of the piezoelectric actuator does not have any curvature. SOLID5 is a type of element that occupies three-dimensional space. It has eight nodes. Each node has three displacements along x, y, and z axis, respectively. A prism-shaped element is formed by defining duplicate node numbers [17].

The SOLID5 element is capable of modeling seven different types of disciplines. When this particular type of discipline is chosen, ANSYS will only consider the behaviors of SOLID5 in u_x , u_y , u_z and volt degrees of freedom. It should be noted that u_x , u_y , u_z indicate the displacements in the x, y and z directions (x, y and z axes are based on the global coordinate system), while volt indicates the difference in potential energy of the electrical particles between two locations [17].

5.3 The Finite Element Formulation for Piezoelectric Materials.

Coupled field elements which consider structural and electrical coupling are required in order to perform the FE analysis of piezoelectric smart structures. The coupled field element should contain all necessary nodal degrees of freedom. The piezoelectric-FE formulation used in ANSYS is briefly described in the following.

Allik & Hughes (1970) laid a foundation of the mathematical procedure of ANSYS in solving a piezoelectric material problem. They considered a linear theory of piezoelectricity. The linear theory of piezoelectricity is a theory in which the elastic, piezoelectric, and dielectric coefficients are treated as constants. Constitutive equations that ANSYS use to model piezoelectric materials [17]:

$$\begin{aligned} \{T\} &= [c]\{S\} - [e]\{E\} \\ \{D\} &= [e^T]\{S\} + [\epsilon]\{E\} \end{aligned} \quad (11)$$

where $\{S\}$ is strain vector, $\{T\}$ is stress vector is the electric displacement, $\{E\}$ is the electric field vector, $[e]$ are the piezoelectric stress matrix, $[c]$ are the

Elastic stiffness matrix at constant electric field and $[\epsilon]$ is the dielectric matrix at constant mechanical strain. Subscripts T denotes matrix transposition [18].

rearranged in matrix form as the following:

$$\begin{Bmatrix} \{T\} \\ \{D\} \end{Bmatrix} = \begin{bmatrix} [c] & [e] \\ [e^T] & [-\epsilon] \end{bmatrix} \begin{Bmatrix} \{S\} \\ \{-E\} \end{Bmatrix}$$

Therefore, ANSYS only considers these material properties for piezoelectric 3-D elements, including compliance matrix, piezoelectric matrix, and permittivity matrix given below:

The Elasticity matrix:

$$c = \begin{bmatrix} c_{11} & c_{12} & c_{13} & 0 & 0 & 0 \\ c_{12} & c_{22} & c_{23} & 0 & 0 & 0 \\ c_{13} & c_{23} & c_{33} & 0 & 0 & 0 \\ 0 & 0 & 0 & c_{44} & 0 & 0 \\ 0 & 0 & 0 & 0 & c_{55} & 0 \\ 0 & 0 & 0 & 0 & 0 & c_{66} \end{bmatrix}$$

The piezoelectric matrix:

$$e = \begin{bmatrix} 0 & 0 & d_{31} \\ 0 & 0 & d_{32} \\ 0 & 0 & d_{33} \\ 0 & d_{24} & 0 \\ d_{15} & 0 & 0 \\ 0 & 0 & 0 \end{bmatrix}$$

coupling

The dielectric matrix:

$$\epsilon = \begin{bmatrix} \epsilon_{11} & 0 & 0 \\ 0 & \epsilon_{22} & 0 \\ 0 & 0 & \epsilon_{33} \end{bmatrix}$$

permittivity

For a piezoelectric-FE, using element shape functions and nodal solution variables can approximate the displacements and electrical potentials within the element domain

$$\{u_c\} = [N^u]^T \{u\}$$

$$V_c = \{N^V\}^T \{V\}$$

$\{u_c\}$ = acements within element domain in the x, y, z directions

V_c = electrical potential within element domain

$[N^u]$ =rix of displacement shape functions

$\{N^V\}$ = or of electrical potential shape functions

$\{u\}$ = tor of nodal displacements

$\{V\}$ = tor of nodal electrical potential

Expanding these definitions:

$$[N^u]^T = \begin{bmatrix} N_1 & 0 & 0 & N_n & 0 & 0 \\ 0 & N_1 & 0 & \dots & 0 & N_n \\ 0 & 0 & N_1 & 0 & 0 & N_n \end{bmatrix} \quad (16)$$

$$\{N^V\}^T = (N_1, N_2, \dots, N_n)$$

where N_i is the shape function for node i

$$\{u\} = [U_{x1}, U_{y1}, U_{z1}, \dots, U_{xn}, U_{yn}, U_{zn}]^T$$

$$\{V\} = \begin{Bmatrix} V_1 \\ V_2 \\ \vdots \\ V_n \end{Bmatrix}$$

where n is the number of nodes of the element

Then the strain $\{S\}$ and electric field $\{E\}$ are related to the displacements and potentials,

$$\{S\} = [B_u] \{u\} \quad (20)$$

$$\{E\} = -[B_v] \{V\}$$

$$[B_u] = \begin{bmatrix} \frac{\partial}{\partial x} & 0 & 0 \\ 0 & \frac{\partial}{\partial y} & 0 \\ 0 & 0 & \frac{\partial}{\partial z} \\ \frac{\partial}{\partial y} & \frac{\partial}{\partial x} & 0 \\ 0 & \frac{\partial}{\partial z} & \frac{\partial}{\partial y} \\ \frac{\partial}{\partial z} & 0 & \frac{\partial}{\partial x} \end{bmatrix}$$

$$[B_v] = \begin{Bmatrix} \frac{\partial}{\partial x} \\ \frac{\partial}{\partial y} \\ \frac{\partial}{\partial z} \end{Bmatrix} \{N^V\}^T$$

The mechanical response of piezoelectric elements can be described by the equation of motion [19].

$$\ddot{\mathbf{u}} \{\text{div}[\mathbf{T}] + \mathbf{f} = \rho\{\ddot{\mathbf{u}}\}$$

Where \mathbf{T} , \mathbf{f} , ρ and $\ddot{\mathbf{u}}$ are stresses, body force in unit volume, density and accelerations, respectively. On the other hand, the electrical response of piezoelectric elements can be expressed by Maxwell's equation

$$\left\{ \frac{\partial \mathbf{D}}{\partial \mathbf{x}} \right\} = \{0\}$$

Where \mathbf{D} is the electric displacement.

With the application of variation principles on the mechanical equilibrium equation, Equation (22) and the electrical flux conversation equation, Equation (23), in conjunction with the approximate field of equation (14, 15, 22, 21) and the constitutive properties given in Equation (11), the piezoelectric FE formulation can be derived in terms of nodal quantities:

$$\begin{bmatrix} [\mathbf{M}] & [\mathbf{0}] \\ [\mathbf{0}] & [\mathbf{0}] \end{bmatrix} \begin{Bmatrix} \{\ddot{\mathbf{u}}\} \\ \{\ddot{\mathbf{V}}\} \end{Bmatrix} + \begin{bmatrix} [\mathbf{C}] & [\mathbf{0}] \\ [\mathbf{0}] & [\mathbf{0}] \end{bmatrix} \begin{Bmatrix} \{\dot{\mathbf{u}}\} \\ \{\dot{\mathbf{V}}\} \end{Bmatrix} + \begin{bmatrix} [\mathbf{K}] & [\mathbf{K}^z] \\ [\mathbf{K}^z]^T & [\mathbf{K}^d] \end{bmatrix} \begin{Bmatrix} \{\mathbf{u}\} \\ \{\mathbf{V}\} \end{Bmatrix} = \begin{Bmatrix} \{\mathbf{F}\} \\ \{\mathbf{L}\} \end{Bmatrix}$$

where, $[\mathbf{M}]$ is the mass matrix derived from density and volume, Structural damping matrix $[\mathbf{C}]$, vector variables \mathbf{u} and \mathbf{V} express structural and electrical degrees of freedom. $[\mathbf{K}]$ is the mechanical stiffness matrix derived from elasticity matrix, $[\mathbf{K}^z]$ is the piezoelectric stiffness matrix derived from piezoelectric matrix, $[\mathbf{K}^d]$ is the dielectric stiffness matrix derived from dielectric matrix. The variables \mathbf{F} and \mathbf{L} are the mechanical force vector and charge vector, respectively.

$[\mathbf{M}]$, $[\mathbf{K}]$, $[\mathbf{K}^z]$ and $[\mathbf{K}^d]$ matrices are expressed as:

Structural mass matrix:
$$[\mathbf{M}] = \int_v \rho [\mathbf{N}^u] [\mathbf{N}^u]^T dv \quad (25)$$

Structural stiffness matrix:
$$[\mathbf{K}] = \int_v [\mathbf{B}^u]^T \mathbf{c} [\mathbf{B}^u] dv \quad (26)$$

Piezoelectric coupling matrix:
$$[\mathbf{K}^z] = \int_v [\mathbf{B}^u]^T \mathbf{e} [\mathbf{B}_v] dv$$

Dielectric conductivity matrix:
$$[\mathbf{K}^d] = \int_v [\mathbf{B}_v]^T \boldsymbol{\epsilon} [\mathbf{B}_v] dv$$

Structural damping matrix $[\mathbf{C}]$ can be defined as linear combination of mass and mechanical stiffness matrices as

$$[\mathbf{C}] = \alpha[\mathbf{M}] + \beta[\mathbf{K}]$$

Where the variables α and β are the Rayleigh damping coefficients.

Energy coefficients are calculated for each piezoelectric element as follows:

Elastic energy:
$$U_E = 1/2 \{S\}^T [e] \{S\}$$

 Dielectric energy:
$$U_D = 1/2 \{E\}^T [\epsilon] \{E\} \quad (31)$$

Electromechanical coupling energy:
$$U_M = -1/2 \{S\}^T [e] \{E\} \quad (32)$$

Potential energy:
$$E^P = U_E + U_D \quad (33)$$

5.4 Closed Loop System

LQR gain is considered in this study as the control scheme for controlling the vibration of flexible pipe system. The block diagram of AVC system is shown in Fig. (4). In this figure, G_a , G , G_s and K are the transfer functions of actuator, flexible pipe, sensor and controller gain respectively. Generally, the controller will try to reduce the error between the reference value and its actual value until minimum error is achieved. The effectiveness of the controller action depends on the optimum setting of its parameters or LQR gain [20].

For the closed loop system in Fig. (4), the reference input, which is the desired deflection, is set to zero in order to achieve zero cancellation. The input to the actuator is $-G_s K X$ and its output is thus $F_a = -G_a G_s K X$. Then the total force fed into the system is given by:

$$F = F_d + F_a = F_d - G_a G_s K X \quad (34)$$

Thus, the output of the system which is the deflection of the plate, X can be expressed as:

$$X = G F_d \left(\frac{1}{1 + G_a G_s G K} \right) \quad (35)$$

From equation (35), the deflection of the plate can be reduced by adjusting the controller gain, K . By increasing the controller parameter, the lateral displacement of X will decrease, thus suppressing the amplitude of the vibration. Theoretically, if the value of K is large, the factor $1/(1 + G_a G_s G K)$ will tend to zero. It means that the controller can cope with any disturbance or parameter changes in the dynamics system. This type of controller is quite similar with high gain feedback regulator [21].

For the purpose of simulation, the transfer function for linear actuator and linear sensor is assumed to be unity. Thus the deflection of the plate becomes:

$$X = G F_d \left(\frac{1}{1 + G K} \right) \quad (36)$$

Based on equation (36), the deflection of the plate is inversely proportional to the value of controller gain, K . Thus, the amplitude of oscillation of the plate is reduced by increasing the controller gain, K .

5.5 Closed Loop System

In this section, the active vibration control in smart structures is simulated by ANSYS. The block diagram of the analysis is shown in Fig. (5).

K , and K_v are control and power amplification factors, respectively. K_v is taken 32V by experimental work, and is changed in the analyses below. Only the proportional control is applied. The multiplication of K K_v is the proportional constant for the actuator voltage, V_a . Therefore, changing the values of K and K_v and keeping their multiplication the same do not affect the results. The calculated deflection at a location, X , is observed to evaluate the performance of the vibration control.

5.6 The FE model of Aluminum Pipe and piezoelectric patch

Firstly the analyses is performed using ANSYS FSI workbench then the fluid pressure results transfer into ANSYS parametric design language (APDL). The FE model is created using SOLID45 and SOLID5 for the aluminum pipe and the piezoelectric patch Respectively as shown in Fig. (6 a and b) while Detail of the model PZT patches with electrode shown Fig. (6c) .

Different boundary conditions are applied to the FE model. The FE model of the pipe and PZT is shown in Fig. (6 a and b). The FE model contains 1980 elements and 4226 nodes where this elements numbers are decided after a convergence study made for the ANSYS model.

5.6 Active Vibration Control under Harmonic Excitation

In this section, the active control of a smart pipe under forced vibration is analyzed. The smart pipe is composed of five piezoelectric (Lead- Zirconate-Titanate) patches. Three of the piezoelectric patches are used as two actuator and one sensor while the other piezoelectric patch is used as vibration generating shaker. The smart pipe is harmonically excited by the piezoelectric shaker at its fundamental frequency. The PZT sensor is utilized to sense the vibration level. Active vibration reduction under harmonic excitation.

Harmonic excitation is provided by the piezoelectric vibration generating shaker. The harmonic excitation $vh = asin(\omega t)$ is created with the ANSYS script "Sine.txt" as below.

```
! -----Sine.txt-----
*dim,t,,ny ! Define arrays with dimension
*dim,b,,ny
*dim,c,,ny
*dim,vh,,ny
*vfill,t(1),ramp,0,dt ! Array t(ny) : time in second
*vfact,w ! Multiplying factor: frequency=(2*pi*f1)
```



```
*vfun,b(1),copy,t(1) ! Result array b(n)=frequency*t(ny)
*vfun,c(1),sin,b(1) ! Array c(n)= sin(b(ny))
*vfact,a ! Multiplying factor: amplitude a
*vfun,vh(1),copy,c(1) ! Array vh(ny)= a*c(ny)
```

The parameters n_y , w , a are the number of samples, the circular frequency and the amplitude for the sine wave, respectively. The number of samples depends on the duration of the excitation. The excitation frequency equals to its fundamental natural frequency calculated from the modal analysis. The amplitude of the excitation is taken as 190 V. The time step is also found as $\Delta t=1/f_1/20$ using the first natural frequency. The parameters b and c are temporary arrays to be able to calculate the excitation (vh).

5.6.1 Closed Loop for force vibration

Active control is achieved with the integration of control actions into the FE analysis [22]. The block diagram of the closed loop control is given in Fig. (7).

Control actions are performed with the script code after the FE model of the smart plate is constructed. The analysis of active control is carried out by the following scripts.

```
d,p5,volt,vh
d,p4,volt,vh
time,dt
solve
Ref=0
*do,i,2,ny
d,p4,volt,vh(i)
d,p5,volt,vh(i)
*get,uz,node,p1,u,z
dis= ks *dis
err=Ref-ks *dis
va=k*kv*err
d,p2,volt,va
time,i*dt
solve
*enddo
finish
```

Harmonic excitation is created in the file “sine.txt” before the control loop is initiated. The first step is solved applying the excitation voltage to the piezoelectric shaker. Active control is realized in “*do-*enddo” loop.

6. Experimental Work

6.1 Experimental Rig.

The rig consists of two main parts; the foundation and the Substrate. It was constructed from (120cmx40cmx1cm) rectangular section iron plate foundation and (22cmx20cmx1cm) Substrate of pipe support as shown in Fig.(8).

The clamped support verification by two ball-bearing (Separated by a distance of 3 cm) were used to insure zero slope and displacement necessary for clamped end condition, see Fig.(9).

6.2 Water Circuit.

In all tests, water was used as a flowing fluid .To measure the water flow rate a flowmeter was fitted at the inlet of the test model. The water circuit is shown in Fig.(10). The main components of this circuit are the collecting

tank (150 Lit.), centrifugal pump (100 Lit/min., 25 m), control valve (gate type) and the test pipe model.

7. Hardware Devices

The hardware devices for active vibration control are illustrated as the following:

7.1 Sensor, Actuator and Shaker

QUICKPACK MIDE QP20W double layer piezoelectric type is use as structural sensors transducers, actuator and shaker attaching them either directly to a data acquisition device. Piezoelectric shall be attached to the main structure by special piezoelectric adhesive. This type of piezoelectric can be used as sensor and actuator at same time.. The transducers come in a convenient pre-packaged form, along with the electrodes and a connector block. A QP20W transducer is shown in Fig.(11a) [23].

The type of transducer used in this work is suitable for strain actuation. It consists of two piezoelectric wafers, made of PZT5A. The dimensions of the wafer are $45.97 \times 33.02 \times 0.76$ mm and the full-scale voltage applicable is ± 200 V. The nominal device capacitance is 145 nF. The manufacturer gives a $\pm 400\mu\epsilon$ full-scale strain. The material properties of PZT shown in Table(1).

The transducers are bonded to the pipe surface using a special structural epoxy resin shown in Fig(11a).

7.2 High Voltage Power Amplifiers.

A power amplifier drives piezoelectric actuators through an applied voltage. The device used in the series of experiments featured in this work is a (Trek Model 2205) high voltage inverted operational amplifier, shown in Fig. (11b) .The device accepts an input signal and amplifies it up to ± 500 V_{peak}.It is stable to drive large capacitive loads, like piezoelectric actuators. It provides an output bandwidth of 75 kHz with 3 dB attenuation . Output Current Range ± 80 mA peak AC for 5ms minimum. The device provides safety measures against overloading the actuators, since too much power and high voltage may damage the piezoelectric devices and the amplifier circuitry. The maximal output power of the amplifier is 40 W [24].

7.3 Data Acquisition.

The National Instruments DAQPad-6015/6016 data acquisition (DAQ) devices provide plug-and-play connectivity via USB for acquiring, generating, and logging data in a variety of portable and desktop applications. DAQPad devices with screw terminals or BNC connectors provide direct connectivity so you can easily connect sensors and signals without extra cost. With DAQPad-6015/6016 mass termination, you can cable to external accessories and signal conditioning devices such as NI SCC devices. All devices feature 16-bit accuracy at up to 200 kS/s. The DAQPad-also provides 32 digital I/O lines for applications requiring an extended interface to digital sensors and actuators. NI-DAQ provides a seamless interface to LabVIEW, LabWindows/CVI. [25]. Photograph of this device shown in Fig.(11c).

7.4 Function Generator

BK model 4075, a 25 MHz arbitrary/Function generator, is a precision source of sine, triangle, square and pulse waveforms plus dc voltage. All can be externally modulated. Output can be continuous or can be triggered or gated by external signal or front panel switch. Amplitude of the waveforms is variable from 30 V down to 1.5 mV. DC reference of the waveform can be offset positively or negatively[25]. Photograph of this device shown in Fig.(11d).

7.5 Oscilloscope.

The digital oscilloscope 250MHz type GW-INSTEK GDS3000 is used with built-in FFT analyzer. This device is used to display the vibration waves and frequency results, which extract from the sensor, due to vibration of the structures.A 100GSa/s ET sampling rate (10ps pt-pt resolution) is provided to accurately reconstruct repetitive waveforms avoiding software interpolation distortion. GDS3000 Series gives you full confidence in every acquisition of complex waveform that adheres to high speed circuit design of modern products. The Power Analysis software contains four measurement functions, including Power Quality, Harmonics, Ripple and Inrush Current. The Power Quality analysis function allows the measurements of Voltage, Current, Frequency, Power and other quality related parameters for power source efficiency improvement. Two high speed USB 2.0 Host ports located in both front panel and rear panel are used for easy access of stored data[25]. Photograph of this device shown in Fig.(11e).

8. Experimental Procedures.

8.1 Natural Frequencies Experiments

In this test the cantilever pipe model was employed with 1m length. In measuring the natural frequencies, the test model was subjected to forced vibration under the action of the harmonic force generated by the piezoelectric shaker. The response of the pipe models was measured by the piezoelectric sensor and displayed via the oscilloscope.

In measuring the natural frequencies of any pipe models, the excitation frequency of the piezoelectric shaker is gradually increased from zero observing the response until a sharp amplitude (resonance) is reached. At this instant the frequency is recorded as the first natural frequency. To measure the second natural frequency the piezoelectric shaker frequency is further increased until a second resonance is reached. The same procedures were repeated for the third natural frequency.

The electrical vibration circuit can be divided into two main circuits; the first represents the "excitation side" which consists of: function generator, high voltage power amplifier and vibration exciter (piezoelectric shaker). The second is the "response side" which includes: piezoelectric sensor and oscilloscope, as shown in Fig.(12).

8.1 Active Vibration control Experiments.

A schematic view of the experimental setup as shown in Fig.(13). In the experimental setup, a multifunction analog (NI-DAQ-6016) is used for data acquisition and control active. The PZT shaker excites the pipe by the sine wave signal in resonance state, the output signal from sine generator is sent through BNC cable to TREK 2205 high voltage power amplifier (HVPA) in order to excite the piezoelectric (shaker) patch. The PZT sensor data is sent through BNC cable to analog input DAQ then sensor data appear in (PC+ Lab VIEW program) and sent also to oscilloscope. The input signal to the DAQ is limited by ± 10 V.

Later, the output signal is sent through BNC cable, which is a terminal block by the analog output DAQ after a control signal by Lab VIEW program. Then the control signal is sent to another TREK 2205 high voltage amplifier (HVPA) in order to actuate the actuator PZT patch.

The same procedure is used for active control of free vibration with replace harmonic excitation(shaker) by initial tip displacement.

9. LabVIEW program.

A personal computer and LabVIEW are used for the implementation of active control. LabVIEW program is called as virtual instrument since the appearance and operation imitate physical instruments. LabVIEW contains a comprehensive set of tools for acquiring, analyzing, displaying and storing data. LabVIEW program consists of two stages such as a block diagram and a front panel. The block diagram contains the code and the front panel is a user interface having controls and indicators.

LQR control programs is developed by LabVIEW (version 12.0) in the experiment as shown in Fig.(14). Control OFF and Control ON signals obtained by LabVIEW program as shown in Fig.(15).

The sample codes developed by LabVIEW in the study are given in Appendix B.

10. Results and Discussions.

The results of free vibration, force vibration and active control vibration are investigated for smart cantilever aluminum pipe conveying fluid. First, the natural frequencies and mode shapes are found. Second, active control vibration is applied for free and force vibration by used output feedback control to remove the undesired vibration.

10.1 Natural Frequency & Mode Shape.

The measured natural frequencies for the lowest three modes of aluminum pipe conveying fluid are presented in Tables (2) .. The water flow rate was fixed at 10 and 40 L/min. For comparison purpose the corresponding theoretical and values of the natural frequencies, and the associated errors are given in the following tables. It shows good agreement between these results.

Table (2) indicate to errors between the theoretical and the experimental values of the natural frequencies. This can be attributed to the following:-

- I. It is impossible to provide perfect boundary conditions in practice.
- II. Many sources of errors such as instruments loading, reading,..etc.
- III. Hose connection at the pipe inlet adds additional stiffness to the pipe models.

Fig. (16) shows the mode shapes of a cantilever pipe at 20L/min flow rate

10.2 Active Vibration Control Results

10.2.1 Free Vibration

The same structure in Fig.(1) is analyzed for active control of free vibration at discharge flow rate ($Q=20$ L/min) with two piezoelectric actuators (1,3). The initial Displacement 8mm is applied to the tip of the pipe to

obtain the free vibration.

The experimental of tip displacement responses and actuation voltage at location 1 are shown in Fig. (17), for location 3 are shown in Fig.(18) for the pipe with and without active vibration control (Control OFF & Control ON). The weight matrix q , weight coefficient ($r=1$) and the maximum actuation voltage was 180 volt for all cases.

$$(q = 10^6)$$

Note that from the experimental result of location 3 the settling time for the response to reach steady state reduced from 3 to 2.5 second while for location 1 settling time reduced from 3 to 1 second with less time of actuation voltage due to the maximum strain in this location.

10.2.2 Force Vibration.

The smart structure in Fig.(1) is analyzed for active control of force vibration, LQR Control performances are tested at three different location for constant weight coefficient ($r=1$) and different weight matrix ($q = 10^6, 10^8, 10^{10}$) The PZT shaker is used to produce ± 8 mm steady state displacement at the tip pipe. Vibration responses are obtained with both the simulation and the experiment.

The control action is started at $t=0$ s in order to decrease steady state vibration amplitudes of the smart pipe under harmonic excitation. Actuation voltages become higher if the control actions start in any time after the excitation is applied. The maximum applicable amplitude of the actuation voltage is 200 V due to the PZT limitations.

high sinusoidal voltage amplitude of 100 V was used to drive the pipe at the first mode in order to see clearly the amplitude of vibration by the naked eye. This test was repeated more than ten times for purposes of inspection and was recorded as a video which is attached to the thesis.

LABVIEW picture for the closed loop time responses of sensor and actuator voltage shown in Fig. (19).

Simulation and experimental results in two different flow velocity ($Q=10$ and 40 L/min) are shown in Figures (21 to 24), this figures include the uncontrolled and controlled responses and actuating voltage for three different gain values.

For the uncontrolled responses, the transient parts in the flow rate ($Q=10$ L/min) and ($Q=40$ L/min) take approximately 2 s and 4 s, respectively. For the controlled responses, higher gain provides better reduction in the amplitudes.

The control performance decrease with increasing the flow velocity due to increased coriolis force.

Piezoelectric actuator in location 1 have higher control performance compared with location 3 as well as in location 1 maximum strain is produced therefore the optimal location of piezoelectric is location 1. the mode strain of the pipe shown in Fig.(20)

10. Conclusions.

The main conclusions obtained from the present work are listed below:

1. The experimental results show satisfactory agreement with the theory many aspects of the dynamical behaviour of pipe conveying fluid were observed experimentally such as: the decrease in natural frequencies with increasing of the fluid velocity. Very little effect was observed for the velocity ranges used.
2. The experimental and simulation results of active vibration control show that the location of the piezoelectric actuator affects the displacement response of the mechanical system. Piezoelectric in location 1 have higher control performance and settling time as compared with locations 2 & 3 as well as in location 1 maximum strain and stress is produced therefore the optimal location of piezoelectric is location 1. The results of the experimental work is matching with result obtain by ANSYS Simulation.
3. The experimental response result for the active vibration control of the pipe conveying steady flow in free vibration show that the settling time for the vibration reduced effectively and vibration suppression is obtained for various gains, the maximum reduced settling time was from 3 seconds to 1 second.
4. The control performance decrease with increasing the flow velocity due to increased coriolis force.
5. The better performance of control occur at minimum velocity ($Q=10$ L/min) and location 1 of actuator, the maximum reduced the displacement response from +8mm to 1mm.
6. The material properties and effectiveness of the piezoelectric sensor, actuator and shaker were reduced after bonding. However, the effectiveness of the piezoelectric actuator was reduced after a number of tests and the actuator used for vibration attenuation became completely non-functional, and in addition all values of piezoelectric capacitance were decreased.
7. In this work, the most significant cause of actuator degradation and failure was the activation of the controller after the amplitude of vibration reached the maximum at steady state. This led the controller to produce high peak voltage at activation for a short time (a transient state) which progressively increased actuator degradation and failure. This problem can be eliminated by setting the controller always to the active (ON) condition before drive the pipe at natural frequencies in order to eliminate the effect of high peak voltage.

References

- [1] Baz A, Kim M. "Active Modal control of vortex-induced vibrations of a flexible cylinder" *Journal of Sound and Vibration*, Vol. 165(1), 69-84, 1993.
- [2] Tsai Y k, Lin Y H "Adaptive modal vibration control of a fluid-conveying cantilever pipe" *Journal of Sound and Vibration*, Vol. 535-547, 1997.
- [3] Yau C H, Bajaj A K, Nwokah O D. "Active control of chaotic vibration in a constrained flexible pipe conveying fluid" *Journal of Fluids and Structures*, Vol. 9, 99-122, 1995.
- [4] Lin Yih Hwang, Huang Rui Chong, Chu Chih Liang. "Optimal modal vibration suppression of a fluid-conveying pipe with a divergent mode" *Journal of Sound and Vibration*, Vol. 271, 577-597, 2004.
- [5] Baz A, Poh S. Experimental implementation of the modified independent modal space control. *Journal of Sound and Vibration*, Vol. 139(1), 133-149, 1990.
- [6] Preumont, A. and K. Seto. "*Active Control of Structures*" United Kingdom: Wiley, 2008.
- [7] Manjunath, T.C. and B. Bandyopadhyay "Vibration control of Timoshenko smart structures using multirate output feedback based discrete sliding mode control for SISO systems" *Journal of Sound and Vibration*, Vol. 326(1-2), 50-74, 2009.
- [8] Kumar, K.R. and S. Narayanan "The optimal location of piezoelectric actuators and sensors for vibration control of plates" *Smart Materials and Structures*, Vol. 16(6), 2680-2691, 2007.
- [9] Ramesh Kumar, K. and S. Narayanan "Active vibration control of beams with optimal placement of piezoelectric sensor/actuator pairs" *Smart Materials and Structures*, Vol. 17(5), 2008.
- [10] Balamurugan, V. and S. Narayanan "Active vibration control of piezolaminated smart beams" *Defence Science Journal*, Vol. 51(2), 103-114, 2001.
- [11] Narayanan, S. and V. Balamurugan "Finite element modelling of piezolaminated smart structures for active vibration control with distributed sensors and actuators" *Journal of Sound and Vibration*, Vol. 262(3), 529-562, 2003.
- [12] Kapuria, S. and M.Y. Yasin "Active vibration suppression of multilayered plates integrated with piezoelectric fiber reinforced composites using an efficient finite element model" *Journal of Sound and Vibration*, Vol. 329(16), 3247-3265, 2003.
- [13] Zabihollah, A., R. Sedaghati, and R. Ganesan "Active vibration suppression of smart laminated beams using layerwise theory and an optimal control strategy" *Smart Materials and Structures*, Vol. 16(6), 2190-2201, 2007.
- [14] Uyanik, H. "Active vibration control of a fully clamped laminated composite plate subjected to impulsive pressure loadings", in *Recent Advances in Space Technologies*, 2009. RAST '09. 4th International Conference on, 2009.
- [15] Han, J.H. and I. Lee "Optimal placement of piezoelectric sensors and actuators for vibration control of a composite plate using genetic algorithms" *Smart Materials and Structures*, Vol. 8(2), 257-267, 1999.
- [16] Preumont, A. "Vibration control of active structures an introduction". Netherlands: Kluwer Academic Publishers, 2002.
- [17] ANSYS, 2004. ANSYS user manual, ANSYS, Inc., Canonsburg, USA, (www.ansys.com).
- [18] B. Bandyopadhyay, T.C. Manjunath, M. Umamathy "Modeling, Control and Implementation of Smart Structures, A FEM – State Space Approach", Springer Berlin Heidelberg, New York, USA, 2007.
- [19] Sekouri, E. M. "Modelling and shape estimation of smart structures for active control", Ph.D Thesis. Quebec University, CANADA, 2004.
- [20] P. Gardonio, "Sensor-Actuator Transducers for Smart Panels", Australia 2006.
- [21] A. R. Tavakolpour, M. Mailah and I. Z. Mat Darus, "Active Vibration Control of a Rectangular Flexible Plate Structure Using High Gain Feedback Regulator" *International Review of Mechanical Engineering*, Vol. 3(5), 579-587, 2009.
- [22] Kelly, S. G. "Fundamentals of mechanical vibrations". Singapore. McGraw-Hill, (1993).
- [23] PACKAGED PIEZOELECTRIC ACTUATORS AND SENSORS (Mide QuickPack product)
- [24] Trek Model 2205 Piezo Driver/Power Amplifier.
- [25] Z. Shi, G. Ma, and Q. Hu, "A hybrid control scheme of vibration reduction of flexible spacecraft during attitude maneuver" 1st International Symposium on Systems and Control in Aerospace and Astronautics, pp. 169-174, Jan. 2006.

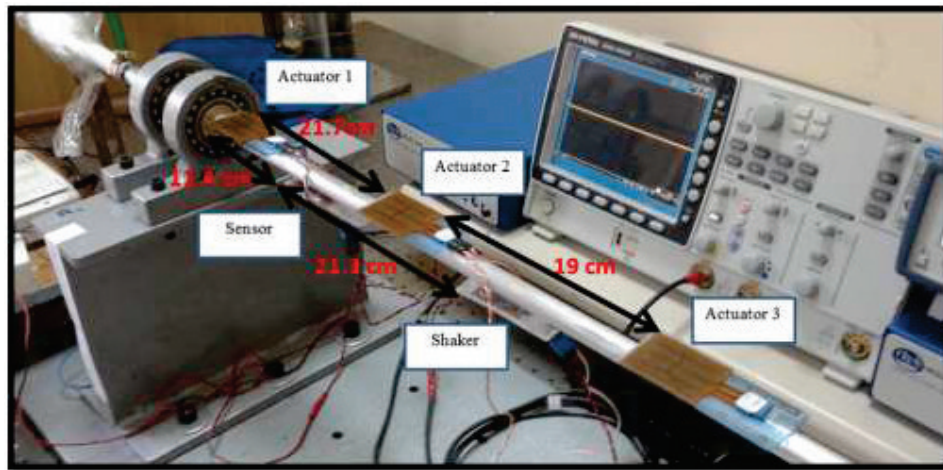
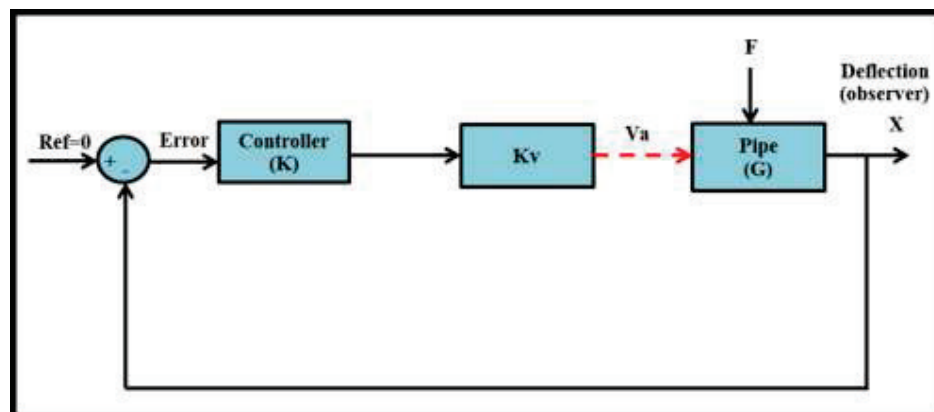


Fig.(1): Modal structure of pipe conveying fluid



Fig.(2) ANSYS workbench (multi-stage work).



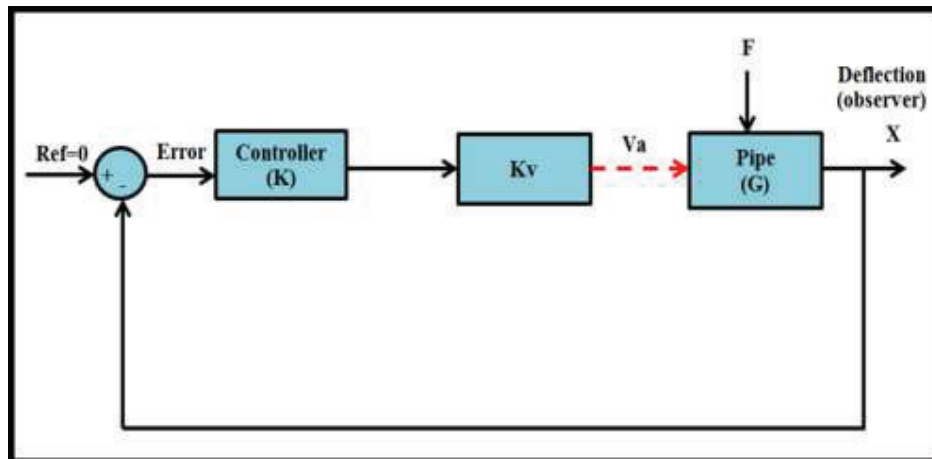
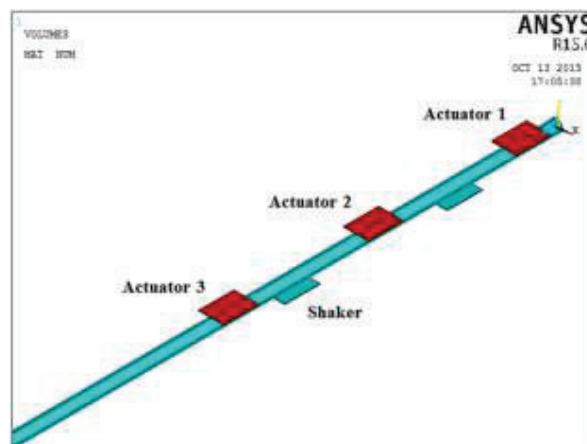
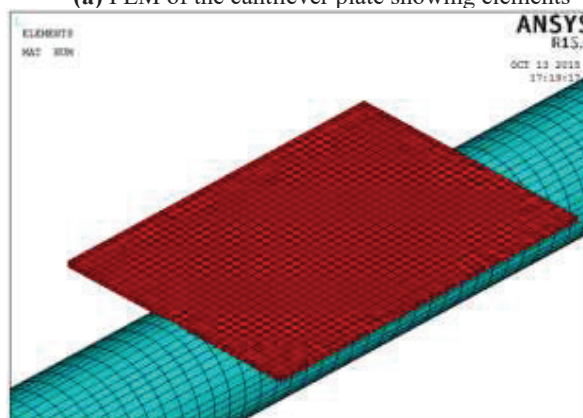


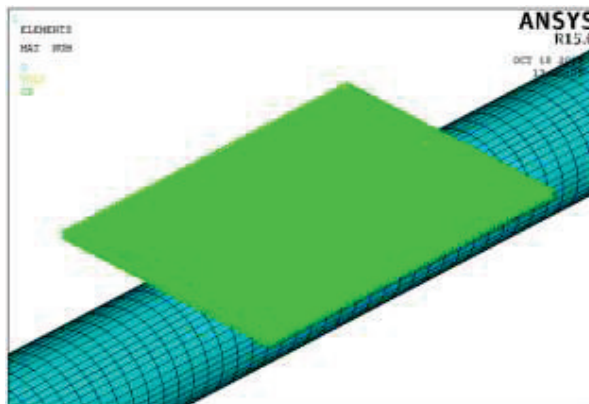
Fig.(5)Block diagram of analysis.



(a) FEM of the cantilever plate showing elements



(b) Detail of the model PZT patches



c) Detail of the model PZT patches with electrode

Fig.(6): The finite element model of the cantilever pipe equipped

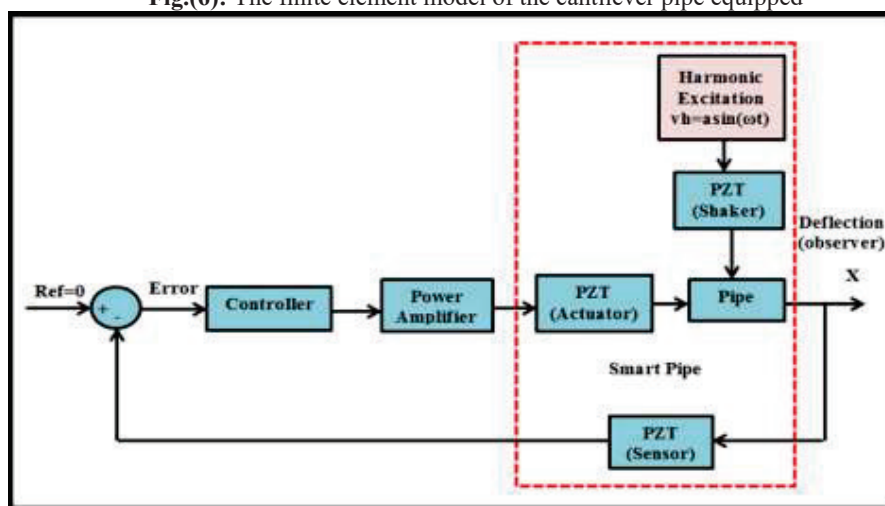


Fig.(7):Block diagram of closed loop control for Harmonic Excitation.

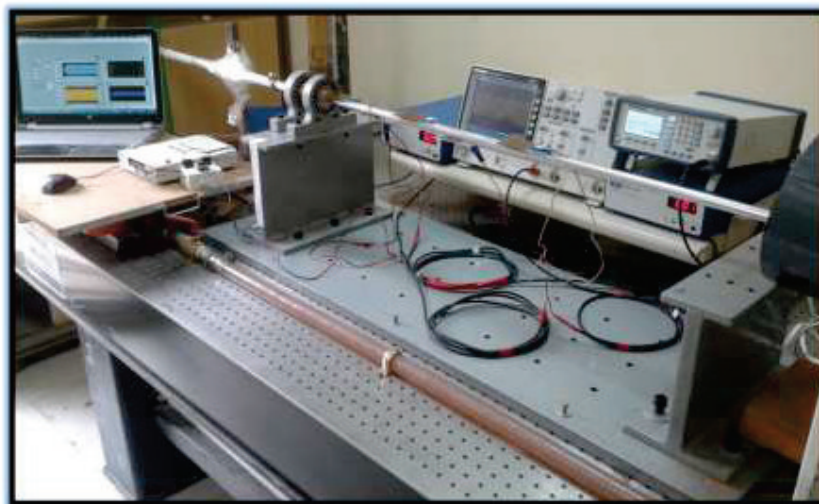


Fig.(8): A photograph of Experimental Rig.

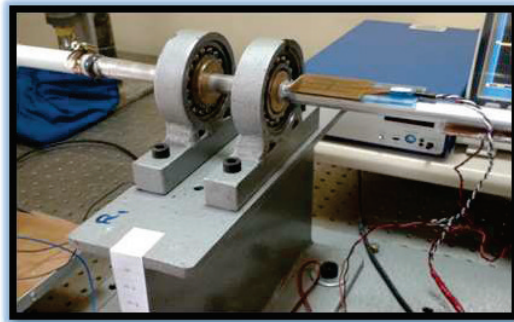


Fig.(9): A photograph of the clamped support.

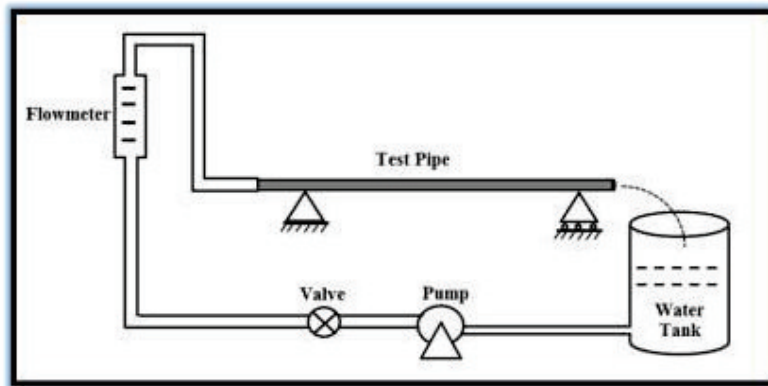


Fig.(10): Schematic diagram of water circuit and the test model



(a)



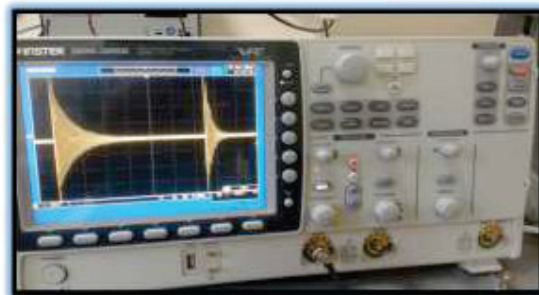
(b)



(c)



(d)



(e)

Fig.(11): A photograph of the Experimental Instruments.

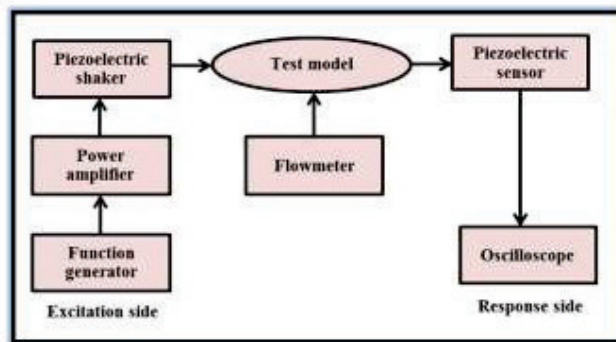


Fig.(12): Block diagram of the measuring circuit

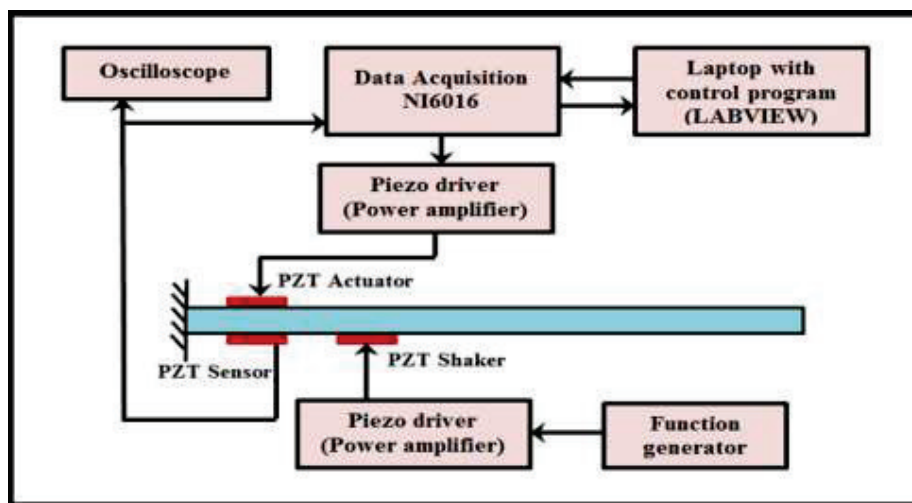


Fig.(13): Block diagram of the electric vibration and control instrument.

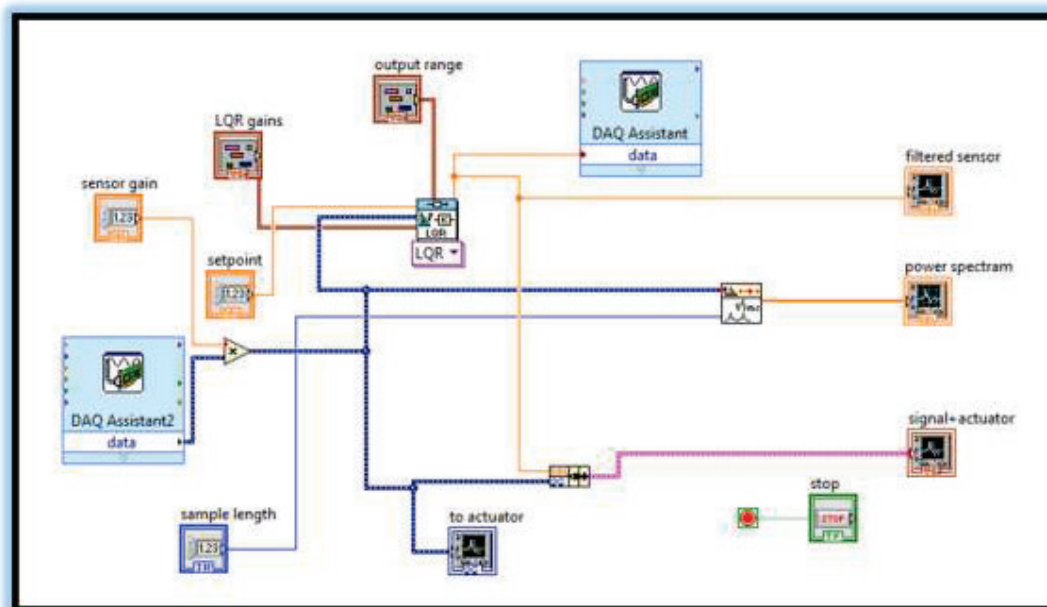


Fig.(14): Block diagram in LabVIEW for LQR control.

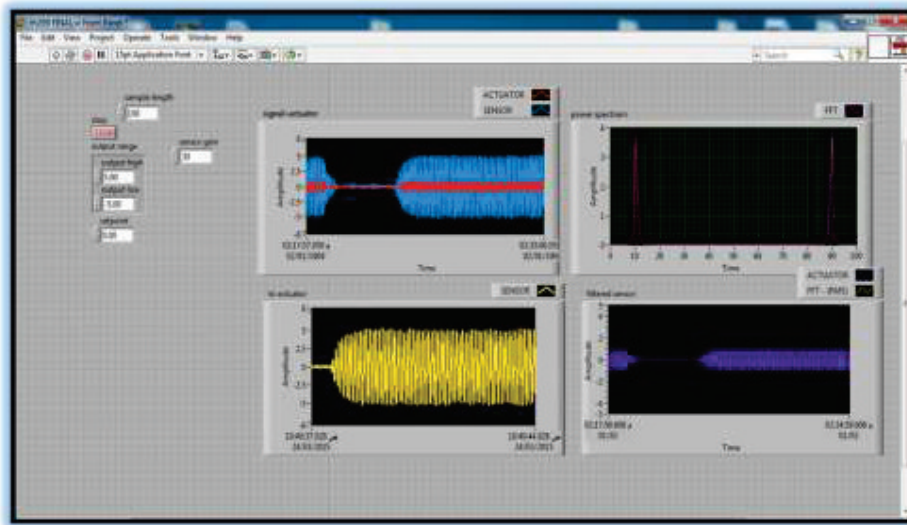
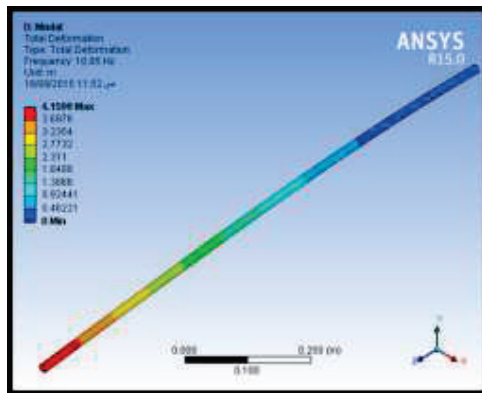
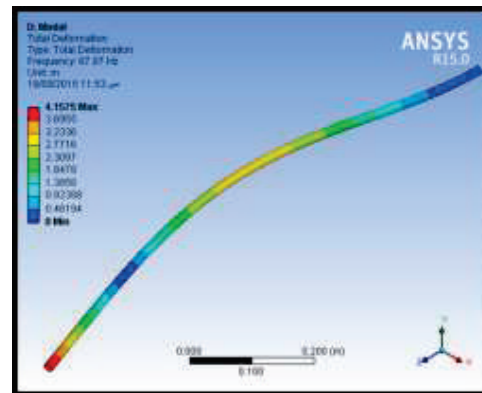


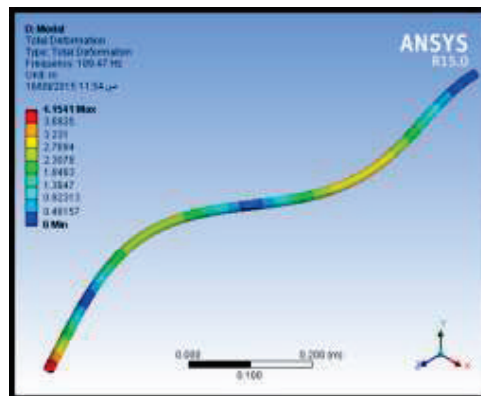
Fig.(15): Control OFF and Control ON signals obtained by LABVIEW program.



(a)First mode shape



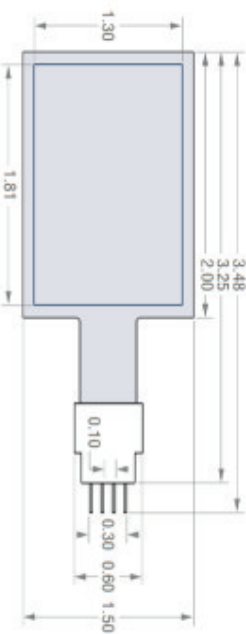
(b)Second mode shape



(c)Second mode shape

Fig.(16): Mode shapes of pipe conveying fluid at 20L/min.

Table(1) : Dimensions and material properties of aluminum pipe and piezoelectric PZT-5A.

<i>Properties</i>	<i>Value</i>	<i>Dimensions</i>
Pipe		
Young modulus(E)	60.8(Gpa)	Outer diameter (0.010 m) Thickness(0.0011 m) Length(1 m)
Density	2590(kg/m ³)	
Piezoelectric		
Young modulus(E)	68x 10 ¹⁰ (N/m ²)	
Density	7750 (kg/m ³)	
Elastic stiffness matrix		
C11	12.1x 10 ¹⁰ (N/m ²)	
C22	12.1x 10 ¹⁰ (N/m ²)	
C12	7.54x 10 ¹⁰ (N/m ²)	
C13	7.52x 10 ¹⁰ (N/m ²)	
C23	7.52x 10 ¹⁰ (N/m ²)	
C33	11.1x 10 ¹⁰ (N/m ²)	
C44	2.11x 10 ¹⁰ (N/m ²)	
C55	2.11x 10 ¹⁰ (N/m ²)	
C66	2.26x 10 ¹⁰ (N/m ²)	
piezoelectric coupling coefficients in the stress-charge		
d31	-5.4 (m/V)	
d32	-5.4 (m/V)	
d33	15.8 (m/V)	
d24	12.3 (m/V)	
d15	12.3 (m/V)	
Dielectric matrix		
ε₁₁	8.11x 10 ⁻⁹ (F/m)	
ε₂₂	8.11x 10 ⁻⁹ (F/m)	
ε₃₃	7.35x 10 ⁻⁹ (F/m)	
		All dimensions are in inches

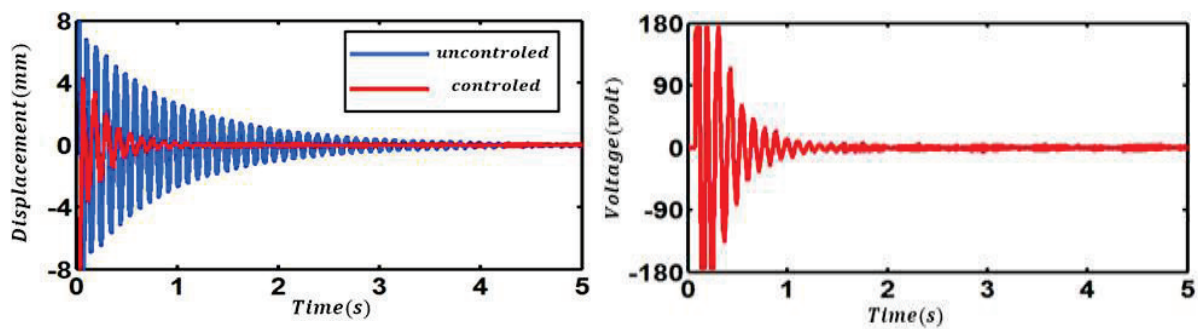


Fig.(17): Experimental results for loaction1.

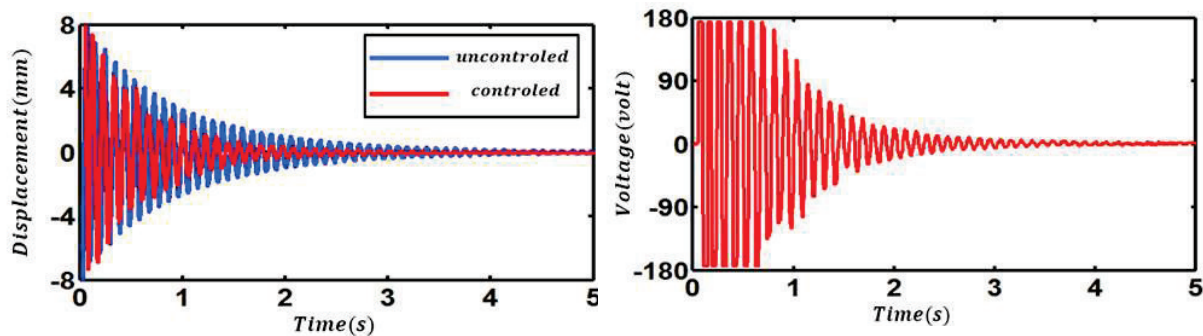


Fig.(18): Experimental results for loaction3.

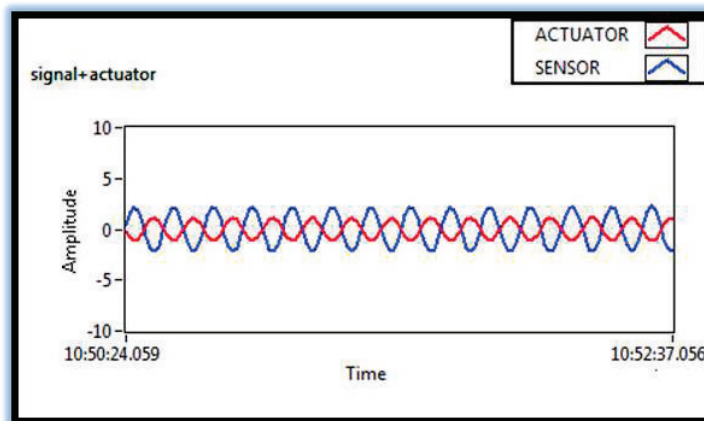


Fig.(19): Steady state closed loop time responses of sensor and actuator feedback voltage.

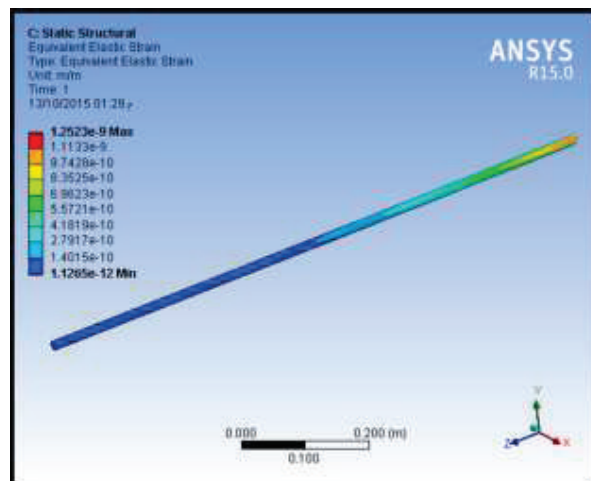
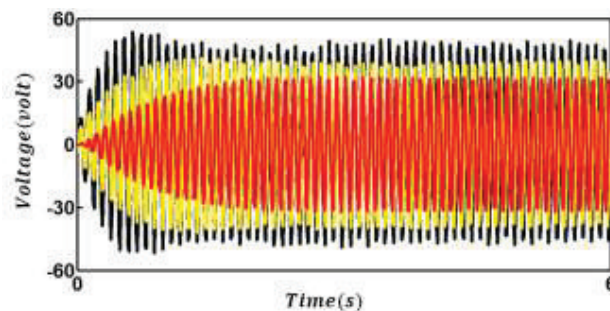
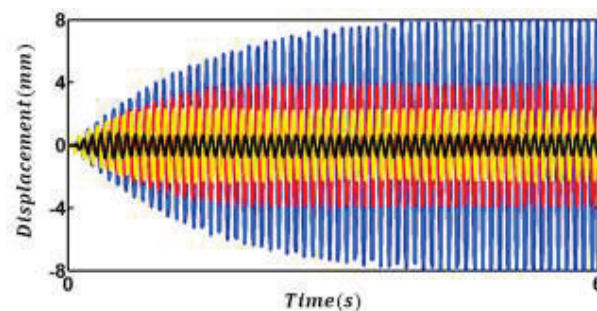


Fig.(20): Mode strain of the cantilever pipe .

Table (2): Experimental and theoretical natural frequencies of pipe conveying fluid

Flow rate(L/min)	Mode No.	Natural frequency (Hz)		%Error
		Experimental	ANSYS	
10	1	10.4	10.6	-1.9
	2	64	67	-4.68
	3	180	190	-5.55
40	1	10.2	10.5	-2.941
	2	62	65	-4.838
	3	175	187	-6.857



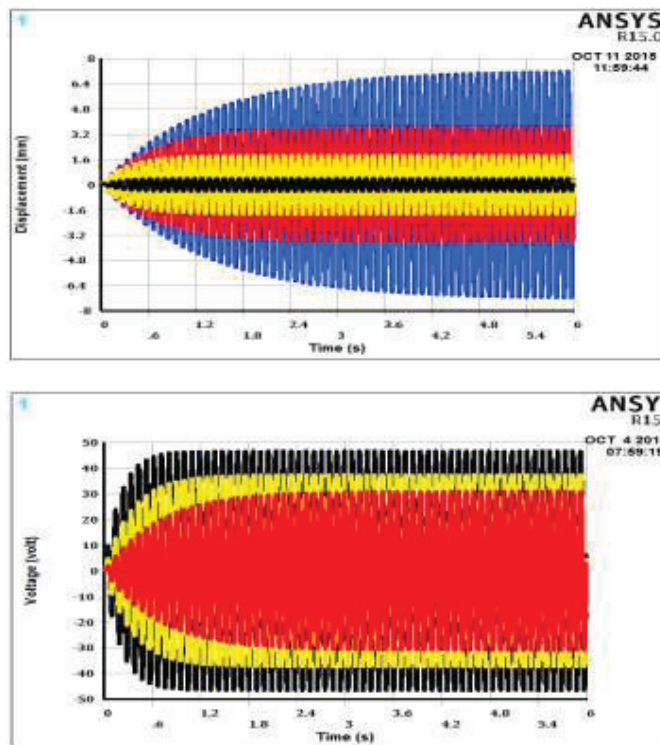
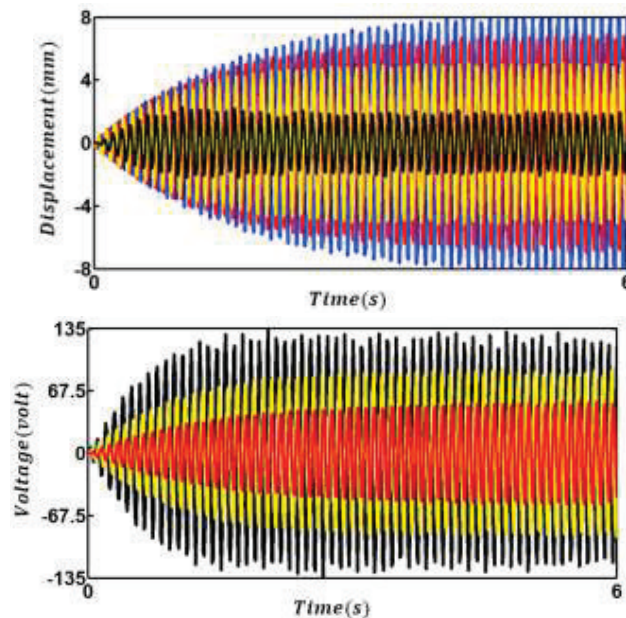
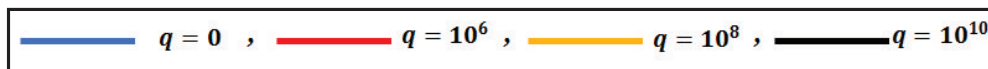


Fig.(21): Experimental and Simulation results for (Q=10L/min, Location 1 of actuator).



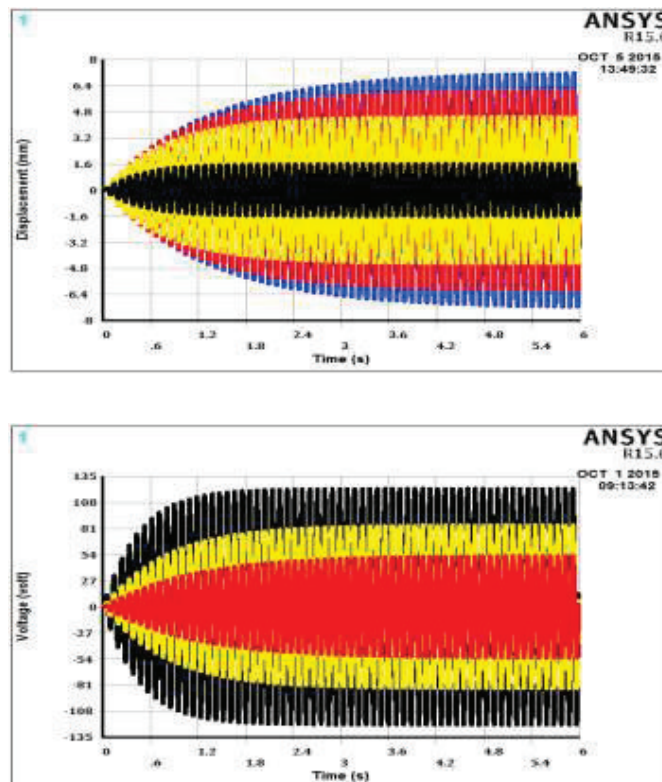
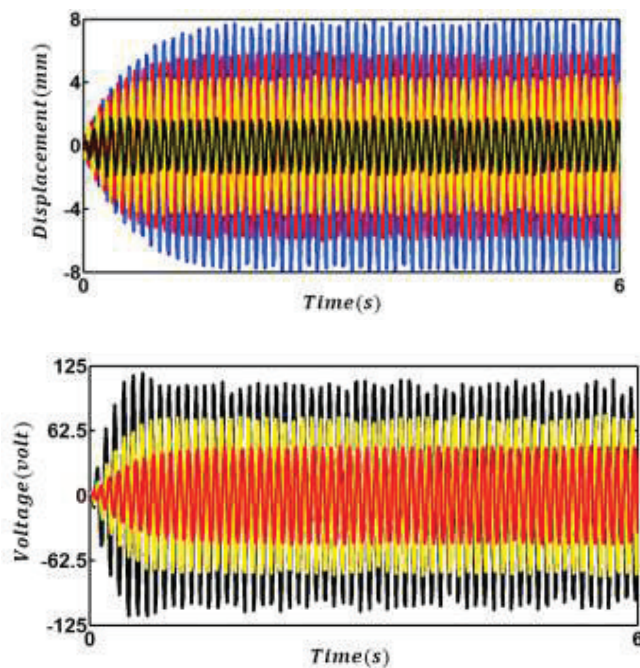
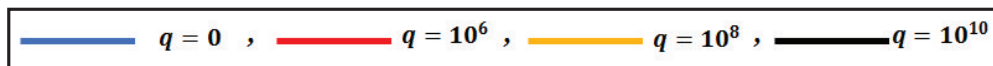


Fig.(22): Experimental and Simulation results for ($Q=10\text{L/min}$, Location 3 of actuator).



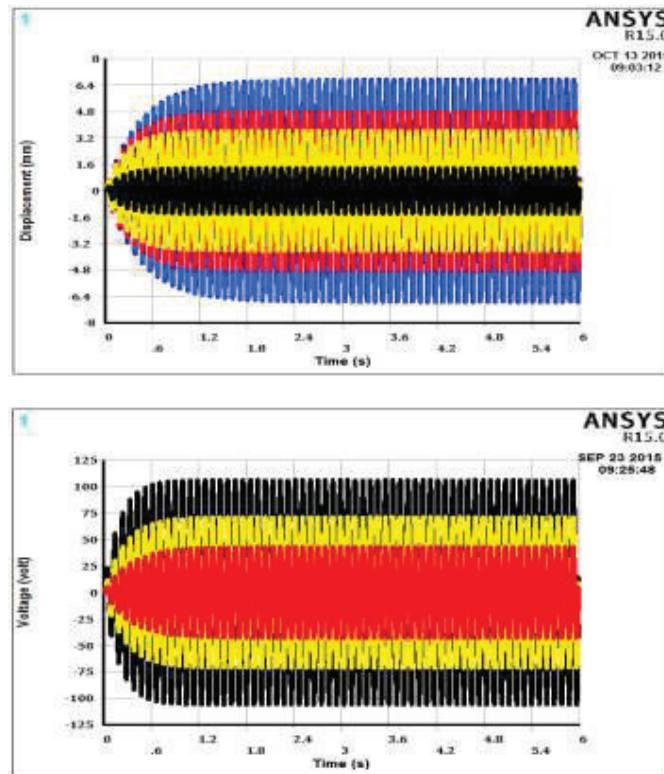
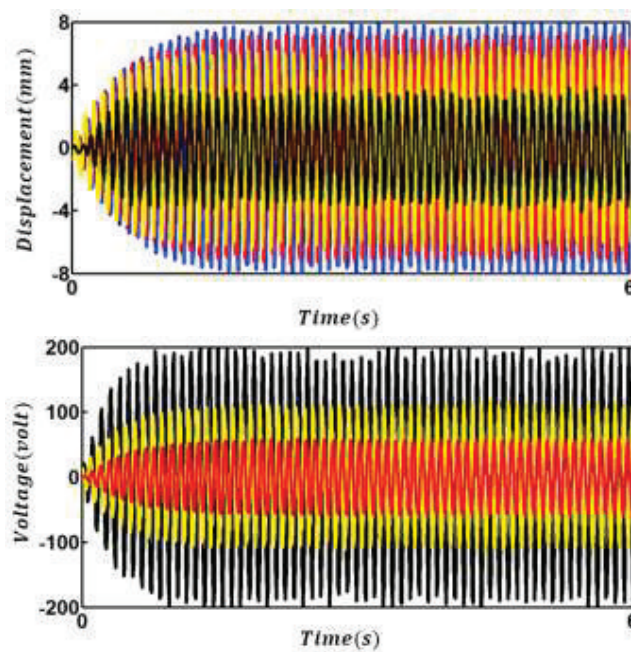
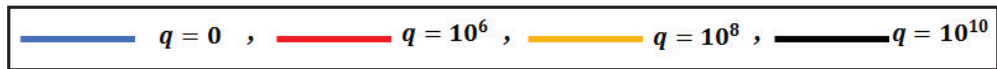


Fig.(23): Experimental and Simulation results for (Q=40L/min, Location 1 of actuator).



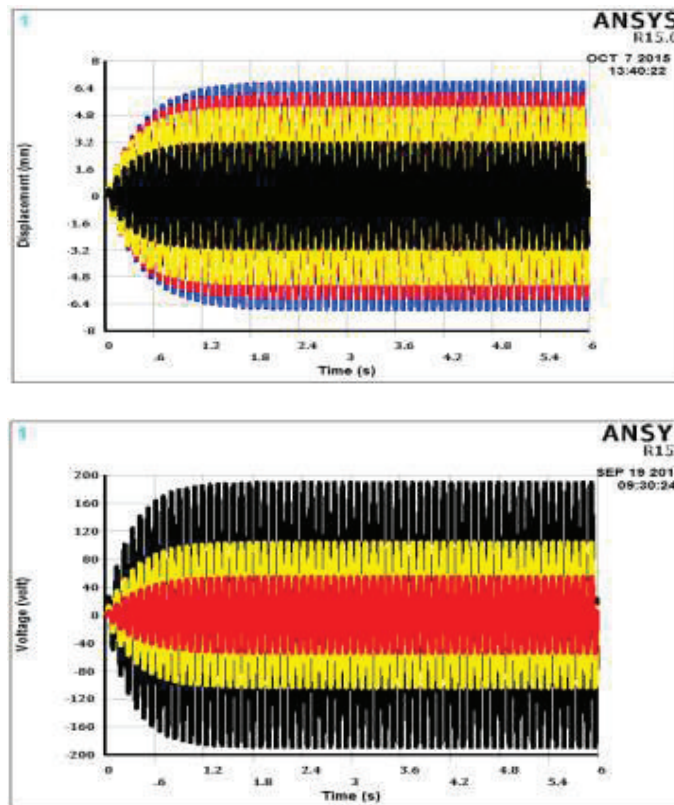


Fig.(24): Experimental and Simulation results for ($Q=40\text{L/min}$, Location 3 of actuator).

